High signal to noise ratio THz spectroscopy with ASOPS and signal processing schemes for mapping and controlling molecular and bulk relaxation processes

Article

Published Version

High signal to noise ratio THz spectroscopy with ASOPS and signal processing schemes for

mapping and controlling molecular and bulk relaxation processes

High signal to noise ratio THz spectroscopy with ASOPS and signal processing schemes for mapping and controlling molecular and bulk relaxation processes

S. Hadjiloucas[1], G.C. Walker[1], J.W. Bowen[1], V.M. Becerra[1], A. Zafiropoulos[2] and R.K.H. Galvão[3]

[1]Cybernetics, School of Systems Engineering, The University of Reading, RG6 6AY, UK
[2]Biosystems Engineering Department, School of Agricultural Technology, Technological Educational Institute of Larissa, 411 10, Larissa, Greece.
[3]Divisão de Engenharia Eletrônica, Instituto Tecnológico de Aeronáutica, São José dos Campos, SP, 12228-900 Brazil.

Correspondance email: s.hadjiloucas@reading.ac.uk

Abstract. Asynchronous Optical Sampling has the potential to improve signal to noise ratio in THz transient sperctrometry. The design of an inexpensive control scheme for synchronising two femtosecond pulse frequency comb generators at an offset frequency of 20 kHz is discussed. The suitability of a range of signal processing schemes adopted from the Systems Identification and Control Theory community for further processing recorded THz transients in the time and frequency domain are outlined. Finally, possibilities for femtosecond pulse shaping using genetic algorithms are mentioned.

1. Introduction
After discussions with A. Bartels of GigaOptics GmbH at an NPL meeting in 2005, where S. Hadjiloucas of Reading University proposed an alternative frequency comb interrogation concept, a dual resonator 35 femtosecond pulse risetime Ti:sapphire prototype spectrometer was developed in Germany to perform THz transient time domain spectrometry (TDS) using an Asynchronous Optical Sampling Scheme (ASOPS) [1-3]. The final system delivered at Reading incorporated large surface area Auston switches with inter-digitated electrodes (TeraSEDs) which were conceptualized in Germany [4], to generate THz pulses from mid-infrared (800 nm) pulses. This scheme can provide an improvement in signal to noise ratio by a factor of 20 when compared to conventional THz transient spectrometers that use the traditional scanning delay line to perform the cross-correlation between pump and probe beams.

An important advantage of eliminating the translation stage from the spectrometer is that the spot size of the optical beam propagating through the reference path of the interferometer is no longer of variable size (due to diffractive spreading of the infrared beam) for different path lengths imposed by the translation stage, as is in the case for a conventional THz transient spectrometer. This is a very important advantage in ASOPS as a dilution of the gate pulse in an Auston receiver changes its multi-moded antenna pattern in both amplitude and phase delay. This type of error has not been

systematically addressed by the THz community although careful work [5] has shown that changing the spot size dramatically alters the recorded time-domain signature and hence the corresponding Fourier transformed spectrum. Such errors are endemic to most THz transient spectrometers and can be exacerbated when ratioing the background and sample spectra.

In addition, although not extensively discussed by the THz community, the THz focusing elements in the system (paraboloids) have also a detrimental effect in the way the radiation propagates through the sample. The beam is diffractively spreading and can no longer be considered as a plane wave incident normally upon the sample. As a consequence, there are cases where not all of the radiation reflected from or transmitted through the sample is detected. One way of gaining further understanding of these phenomena in a quantitative way is to create a full vectorial description of the THz beam incident on the sample and investigate the effect of different degrees of focusing to the observed spectra in a systematic manner. Using information from the focusing elements in the system, the diffractively spreading THz beam can then be represented as a weighted distribution of plane waves incident on the sample over a range of possible angles of incidence [5]. The modification of these plane waves in amplitude, phase and polarisation content should then be propagated through the sample.

Finally, the detection techniques employed in THz TDS are spatially and polarization selective and any sample-induced distortion of the spatial profile and polarization of the THz beam will modify the detected signal in a manner which may mimic absorption and phase delay in the sample [6]. Similar errors are commonly encountered in electro-optic detection schemes, although most of the THz community seems to ignore them.

In the following section, a new inexpensive control loop is suggested for controlling the slave repetition rate laser in ASOPS. In section three, some useful signal processing schemes for THz transients developed over the years are outlined. In section four, a new femtosecond pulse shaping methodology is mentioned. General concluding remarks and applications to these developments are mentioned.

2. Frequency to voltage converter based ASOPS control scheme

Figure 1 depicts the two Verdi-pumped femtosecond Ti:sapphire ring oscillators contained in the GigaJet 20, one of them (slave oscillator) has a mirror mounted on a piezoelectric transducer to control its frequency comb repetition rate at an offset of 20 kHz from the other (master) oscillator.

A schematic of the developed ASOPS THz set-up showing the control loop for the synchronization of the repetition rate of the two femtosecond ring resonators is shown in figure 1. The two femtosecond lasers pumped by two 5 W Verdi lasers produce femtosecond pulses with a repetition rate f and $f + \Delta f$ set by the optical path length of each resonator (around 1 GHz when free running). Using beam splitters, a small portion of the signal (ratio 90:10) is directed to fast photodiodes which produce electrical trigger signals which are further amplified by low-noise high-bandwidth microwave amplifiers (model ZFL 1000LN from Mini-circuits) operated in a trans-impedance configuration (converting a photo-current into a voltage). Although the photodetectors are not preserving the shape of the pulse, this is of no consequence to the stabilization scheme as the goal is to generate a triggering event for the synchronization process. The difference in repetition rate ($\Delta f \approx 20$ kHz) is obtained using a microwave mixer and sent to an AD650 (Analog Devices) frequency to voltage converter (100 kHz full scale with 0.005% linearity) which provides an output between 0 and 10 V. This output is subsequently fed to a SIM 960 analog PID controller (Stanford Research Systems) before being finally sent to a pair of PA240CX (APEX semiconductor) op-amps, connected in a bridge configuration, providing 660 V peak to peak (circuit design implementation as found in Apex Semiconductors Application note 25) to drive the piezoelectric transducer that controls the path length in the slave resonator cavity. The bandwidth of the high voltage amplifier and piezo combination was in excess of 100 kHz ensuring elimination of acoustical noise in the system. For a 30 cm resonator length, the round trip time for a pulse in the resonator is 1 nanosecond.

The designed close-loop system has a large linear gain in the forward path (composed of the cascaded PID signal, high voltage amplifier signal, the transducer voltage to displacement conversion,

and the conversion of resonator path length to frequency comb repetition rate) and unity gain in the feedback path. With reference to figure 1, using transfer function notation and using $A \gg 1$:

$$V_{out} = \frac{A}{1+AB}V_{REF} \approx \frac{A}{AB}V_{REF} = \frac{V_{REF}}{B} \qquad (1)$$

so that the characteristics of the system are governed by the stable characteristics of the feedback path B and the difference in the repetition rate between the two resonators is set by V_{REF}. Controlling the path length in one resonator to one part per thousand (i.e., to a precision of 300 micrometers) using the piezo, therefore, means that a timing jitter of approximately 1 picosecond can be easily achieved with this configuration. This jitter is due to the noise signal at the output of the frequency to voltage converter (which is currently around 10 mV). This can be improved upon with better shielding of the electronics.
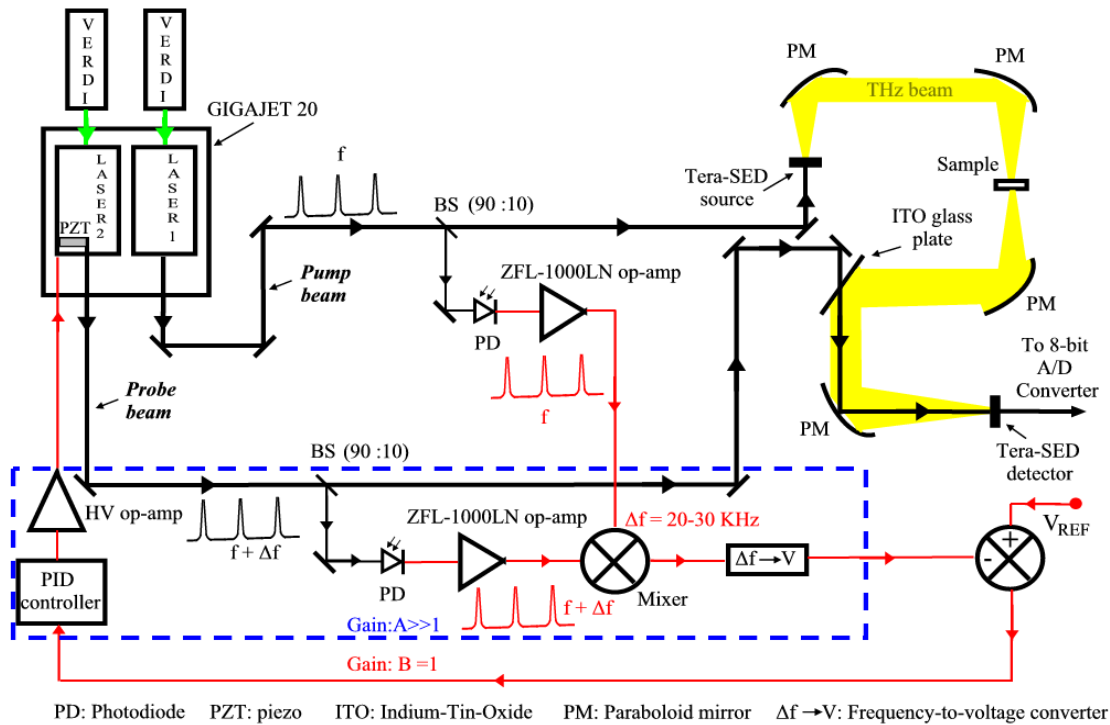

Figure 1. ASOPS THz transient prototype spectrometer based on the GigaOptics Gigajet 20 system and feedback locking scheme.

In figure 1, the overall master-slave repetition rate control scheme is shown. The triggering of the TeraSED detector is performed by the optical pulses from the slave laser. Although two Tera-SEDs are used one for generating and one for detecting the THz transients, it is also possible to use an electro-optic detection set-up (ZnTe crystal and Wollaston prism) with a balanced photodetection scheme to sample the THz transient. The existing 8-bit analog to digital converter used for data acquisition in the current experiments (which is at the front end of the 50 GHz Agilent Infinium oscilloscope we currently use) is not the optimal choice for digitising the observed transients and a dedicated 12 bit or 14 bit data acquisition card with a bandwidth of 100 MHz would be a more appropriate solution to implement, before we can report on the capabilities of the overall system.

3. Signal processing schemes of femtosecond duration transients
In the area of signal processing (de-noising of signals) generated from THz transient spectrometers, we have developed a range of useful algorithms [7,8] to de-embed the complex propagation constant from multi-modal excitation of micro-machined waveguides (useful for micro-spectroscopy applications where the waveguide is filled with small volumes of the dielectric to be characterised). This is achieved by adopting algorithms found in the Systems Identification literature (ARX, and N4SID

Subspace models for linear spectroscopy and NARX models to account for the non-linear cut-on of waveguide modes). Since a femtosecond duration pulse is capable of persistent excitation of the medium within which it propagates, such approach is perfectly justifiable. The multimode Brownian oscillator time-domain response function described by state-space models is a mathematically robust framework that can be used to describe the dispersive phenomena governed by Lorentzian, Debye and Drude responses. In addition, the optical properties of an arbitrary medium can be expressed as a linear combination of simple multimode Brownian oscillator functions.

Additional routines developed at Reading include wavelet filtering [9] of THz transients (using conventional mother wavelets and adaptive structures at each decomposition level), PCA classification schemes [10] and novel apodization structures [11] as the time-domain background and sample interferograms are non-symmetrical. These procedures have useful de-noising properties and can lead to a more precise estimation of the complex insertion loss function.

Current work concentrates on the development of novel system identification tools in the wavelet domain for the further processing of THz transients. Defining the background and sample interferograms as the input and output signals, the frequency response of an identified model would be an estimate of the complex insertion loss (CIL). A wavelet-packet formulation illustrated in figure 2 is adopted and sub-band models $\mathbf{M}_{i,j}(z)$ are identified from the sample and background interferograms by following a least-squares procedure as indicated in figure 3.
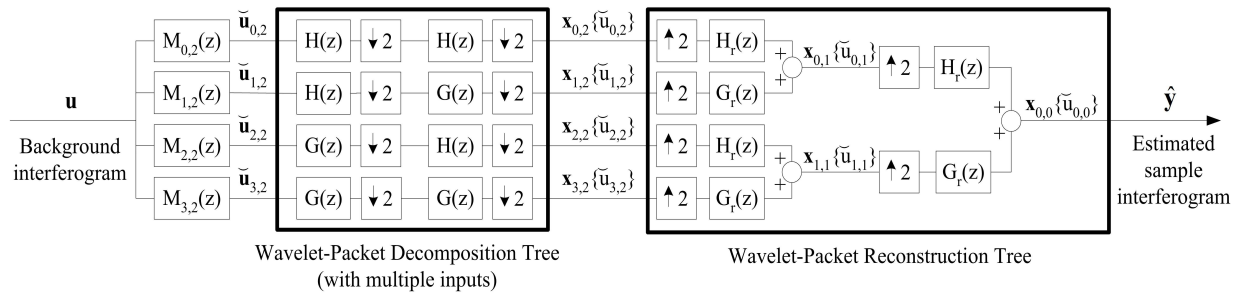

Figure 2. Wavelet-packet model structure. In this example, a complete two-level decomposition tree, which defines four frequency sub-bands, is employed. H(z), G(z) denote low-pass and high-pass decomposition filters, respectively, with reconstruction counterparts represented by $H_r(z)$, $G_r(z)$. The four sub-band models are represented by the transfer functions $\mathbf{M}_{0,2}(z)$, $\mathbf{M}_{1,2}(z)$, $\mathbf{M}_{2,2}(z)$, $\mathbf{M}_{3,2}(z)$.
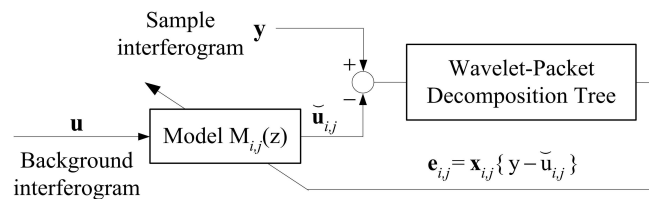

Figure 3. Model identification of a sample interferogram for a given frequency sub-band.

Figure 3 illustrates the procedure adopted to identify each sub-band model $\mathbf{M}_{i,j}$. $\mathbf{u}$ is the input signal used for identification. $\mathbf{y}$ and $\breve{\mathbf{u}}_{i,j}$ are the plant and sub-band model outputs, respectively. Residue $\mathbf{e}_{i,j}$ denotes the wavelet-packet coefficients of the difference between $\mathbf{y}$ and $\breve{\mathbf{u}}_{i,j}$, in the frequency band under consideration. The structure adopted for the sub-band model is a transfer function of the form: $\mathbf{M}_{i,j}(z) = \mathbf{P}_{i,j}(z)\mathbf{Q}_{i,j}(z)$ where $\mathbf{P}_{i,j}(z) = \left(1 - z^{-1}\right)^{-s_{i,j}}$, $s_{i,j} \in \mathbb{Z}$ and $\mathbf{Q}_{i,j}(z) = \alpha_{i,j} + \beta_{i,j}z^{-1}$, with $\alpha_{i,j}, \beta_{i,j} \in \Re$. $\mathbf{P}_{i,j}(z)$ is aimed at roughly approximating the band-limited frequency response of the plant, whereas the Finite Impulse Response (FIR) term $\mathbf{Q}_{i,j}(z)$ provides a fine-tuning for the approximation. A least-squares adjustment for the parameters of $\mathbf{M}_{i,j}$ can be carried out by

minimizing the following cost function $\mathbf{J}_{i,j} : Z \times \Re^2 \to \Re : \mathbf{J}_{i,j}(s_{i,j}, \alpha_{i,j}, \beta_{i,j}) = \mathbf{e}_{i,j}(\mathbf{e}_{i,j})^T$ where $\mathbf{e}_{i,j}$ denotes the row vector of residues for the identification data, as shown in Fig. 3.

4. Genetic algorithms developments for femtosecond pulse shaping experiments

Another line of work at Reading involves the development of a series of evolutionary meta-algorithms in MATLAB, running within the LABVIEW environment to perform pulse shaping of femtosecond duration laser pulses. Proof of principle experiments were performed where the signal from a LABVIEW-controlled function generator was sent to an RF-excited acousto-optic modulator crystal which controls the spectral content and time domain characteristics of 120 femtosecond duration pulses generated from an optically pumped Ti:sapphire Kerr lens mode-locked laser oscillator. The pulses have a useful Fourier transform limited bandwidth of 50-80 nm around a center frequency of 800 nm. The genetic algorithm (GA) population in the developed software consists of a collection of waveforms, each made from two concatenated vectors, one specifying phases over a range of frequencies and the other specifying corresponding magnitudes. Amplitude and phase genes are used to search the evolutionary landscape for desired pulse shapes with specific characteristics. With appropriate pulse shaping schemes realised in pump-probe experiments, it should in principle allow us to control bulk relaxation processes at picosecond timescales.

Selecting a breeding subset from the *N* best fit members (amplitudes and phases) is a very greedy heuristic that often leads to convergence around local optima instead of the global solution. One attempt to circumvent this problem is to use a probabilistic selection of breeding candidates. For instance, with roulette wheel selection (RWS), each member of the population is assigned a slice with an area proportional to fitness. Then, using the proportional probabilities from the roulette wheel, one or two candidates are selected out of the entire population and passed to the operators for production of children. The process is repeated again and again until the desired number of children are created. Because members are never removed from the roulette wheel, members with high fitness are virile and, consequently, they are chosen as parents more frequently than those with low fitness. The process can easily be coded into the algorithm by firstly creating a vector *F* of corresponding fitnesses for the population and then creating a cumulative summed vector for each of all indices in *F*.

As the population starts to converge to a solution, the average fitness of the population will also start to converge to the best fitness. In RWS, the slice size for each population member will be roughly the same size, leaving little differentiation between worst and best fit members. This in turn has a detrimental effect on the selection process, and slows down the convergence of the algorithm considerably. To keep the selection pressure high, we employ fitness scaling and use the scaled fitnesses in RWS instead. This is performed by assigning the best fit member a scaled fitness of 2 and the average fitness a scaled fitness of 1. This way, the best fit member is twice as likely to be chosen as the average fit member.

After measuring and then linearly scaling the fitness, an operator is selected by RWS from a vector of operator weights. Depending on the operator chosen, either one or two parents are selected and then passed on to the operator, thereby creating the child. Initially, the algorithm used seven different operators. Six of these directly exploited the frequency domain: two-point crossover, average crossover, mutation, polynomial phase mutation, creep, and three point smoothing. Current work concentrates in developing a differential evolution scheme and operators in the wavelet domain to perform high resolution waveform matching with a much higher convergence rate.

5. Conclusion

A simple inexpensive control scheme for adjusting the repetition rates of two Ti:sapphire laser oscillators at an offset frequency of 20 kHz has been proposed. The scheme is appropriate for asynchronous optical sampling experiments in THz transient spectrometry, but due to 1/*f* noise and the delay of the frequency to voltage converter in translating the low frequencies into a voltage, it would be less suitable in applications where the offset between the two oscillators must remain at 1 Hz or less [12]. Performance is limited by the linearity of the frequency to voltage chip used in the implementation.

The signal processing of time domain THz transients has been discussed in general terms and a new systems identification approach which can be implemented in the wavelet domain is proposed. The schemes are particularly promising for de-noising purposes as well as in chemometric applications where mixtures of absorbing species are studied.

Finally, a femtosecond pulse shaping methodology is suggested for the optical pulses generated by the femtosecond lasers. The methodology is appropriate for adaptive equalization applications where the goal would be to compensate for dispersion in optical systems such as fibre-optic networks, in high harmonic generation crystals and optical parametric oscillators. Femtosecond pulse shaping techniques in the weak and strong field regimes have the potential to perform mapping of potential energy surfaces in molecular reactions as well as elucidate ultrafast energy transfer dynamics in chemical reactions [13]. Light energy can act as a catalyst to facilitate the progress of molecular and bulk relaxation processes and as a consequence, control the progress of reactions, enabling us to gain further insights in reaction kinetics. Using THz type-setting techniques, there is also the potential to modulate THz transients for very high bit rate communications over short distances.

6. References

[1]   C. Janke, M. Först, M. Nagel, H. Kurtz, and A. Bartels, 2005. 'Asynchronous optical sampling for high-speed characterization of integrated resonant terahertz sensors', *Opt. Lett.,* **30**, 1405-1407.

[2]   A. Bartels, A. Thoma, C. Janke, T. Dekorsy, A. Dreyhaupt, S. Winnerl, and M. Helm, "High-resolution THz spectrometer with kHz scan rates," *Opt. Express* **14**, 430-437 (2006)

[3]   A. Bartels, R. Cerna, C. Kistner, A. Thoma, F. Hudert, C. Janke, and T. Dekorsy (2007) 'Ultrafast time-domain spectroscopy based on high-speed asynchronous optical sampling' *Rev. Sci. Instrum.* **78**, 035107

[4]   A. Dreyhaupt, S. Winnerl, T. Dekorsy, and H. Helm, (2005) "High-intensity terahertz radiation from a microstructured large-area photoconductor," *Appl. Phys. Lett.* **86,** 121114-121111.

[5]   G.C. Walker 2003 '*Modelling the Propagation of Terahertz Radiation in Biological Tissue*' PhD Thesis, Centre of Medical Imaging Research, University of Leeds.

[6]   J.W. Bowen, G.C. Walker and S. Hadjiloucas 2007 'Sample-Induced Beam Distortions in Terahertz Time Domain Spectroscopy and Imaging Systems', *Joint 32nd International Conference on Infrared and Millimetre Waves and 15th International Conference on Terahertz Electronics,* Cardiff, UK 208-209.

[7]   S. Hadjiloucas, R. K. H. Galvão, V. M. Becerra, J. W. Bowen, R. Martini, M. Brucherseifer, H. P. M. Pellemans, P. Haring Bolívar, H. Kurz, J. M. Chamberlain, 2004 'Comparison of state space and ARX models of a waveguide's THz transient response after optimal wavelet filtering,' *IEEE Transactions on Microwave Theory and Techniques*, **52**, 2409-2419.

[8]   R.K.H. Galvão, S. Hadjiloucas, V.M. Becerra and J.W. Bowen, 2005 'Subspace system identification framework for the analysis of multimoded propagation of THz-transient signals,' *Measurement Science and Technolgy*, **16**, 1037-1053.

[9]   R.K.H. Galvão, S. Hadjiloucas, J.W. Bowen and C.J. Coelho, 2003 'Optimal discrimination and classification of THz spectra in the wavelet domain,' *Optics Express*, **11**, 1462-1473.

[10]   S. Hadjiloucas, R.K.H. Galvão and J.W. Bowen, 2002 'Analysis of spectroscopic measurements of leaf water content at THz frequencies using linear transforms,' *Journal of the Optical Society of America A* **19**, 2495-2509,.

[11]   R.K.H. Galvão, S. Hadjiloucas, A. Zafiropoulos, G.C. Walker, J.W. Bowen and R. Dudley 2007 'Optimization of Apodization Functions in THz Transient Spectrometry,' *Opt. Lett.,* **32**, 3008-3010.

[12]   F. Keilmann, C. Gohle, and R. Holzwarth, (2004). 'Time-domain mid-infrared frequency-comb spectrometer', *Opt. Lett.*, **29**, 1542-1544.

[13]   J. Savolainen, N. Dijkhuizen, R. Fanciulli, P.A. Liddell, D. Gust, T.A. Moore, A.L. Moore, J. Hauer, T. Buckup, M. Motzkus, and J.L. Herek (2008) 'Ultrafast Energy Transfer Dynamics of a Bioinspired Dyad Molecule' *J. Phys. Chem. B*, **112** (9), 2678–2685